Mechanisms governing dendritic γ-aminobutyric acid (GABA) release in the rat olfactory bulb

Jeffry S. Isaacson*

Department of Neuroscience, University of California at San Diego School of Medicine, La Jolla, CA 92093-0608

Edited by Richard W. Tsien, Stanford University School of Medicine, Stanford, CA, and approved November 15, 2000 (received for review September 17, 2000)

In the olfactory bulb, synaptic transmission between dendrites plays an important role in the processing of olfactory information. Glutamate released from the dendrites of principal mitral cells excites the dendritic spines of granule cells, which in turn release γ-aminobutyric acid (GABA) back onto mitral cell dendrites. Slow *N*-methyl-D-aspartate (NMDA) receptors on granule dendrites are particularly effective in driving this reciprocal dendrodendritic inhibition (DDI), raising the possibility that calcium influx through NMDA receptors may trigger GABA exocytosis directly. In this study, I show that NMDA receptor activation is not an absolute requirement and that DDI can be evoked solely by α-amino-3-hydroxy-5-methyl-4-isoxazolepropionic acid (AMPA) receptors when granule cell excitability is increased or under conditions that slow AMPA receptor kinetics. In physiological extracellular Mg^{2+}, DDI elicited by photolysis of caged calcium in mitral dendrites is blocked by cadmium and toxins to N- and P/Q-type voltage-gated calcium channels. DDI is largely unaffected after granule dendrites have been loaded with the slow calcium chelator EGTA, suggesting a tight coupling between the site of calcium influx and the release machinery governing GABA exocytosis. These results indicate that voltage-gated calcium channels play an essential role in dendritic GABA release during reciprocal feedback inhibition in the olfactory bulb.

Throughout the central nervous system, neurotransmission occurs primarily when axonal nerve endings release transmitter at synaptic contacts on neural dendrites. However, transmitter release from dendrites underlies synaptic communication in a variety of brain regions (1–3). Dendritic transmission is of particular importance in the olfactory bulb, where olfactory information is first processed in the brain (4). Here, interactions between principal mitral cells and adjacent interneurons, granule cells, are thought to play a major role in the local processing of olfactory information: glutamate released from mitral dendrites excites granule cell spines, which in turn, release γ-aminobutyric acid (GABA) back onto mitral cell dendrites. This reciprocal synaptic arrangement underlies dendrodendritic self-inhibition (DDI) and lateral inhibition of mitral cells (5–9), and these interactions between mitral and granule cells have a central role in odor detection and discrimination (10).

Recent studies indicate that *N*-methyl-D-aspartate (NMDA) receptors (NMDARs) on granule cells have an important action in dendritic GABA release during self- and lateral inhibition (11–14). Because both α-amino-3-hydroxy-5-methyl-4-isoxazolepropionic acid (AMPA) receptors (AMPARs) and NMDARs are believed to be colocalized on granule cell spines (11, 12, 15), why are NMDARs especially good at driving GABA release? One possibility is that the slow kinetics of NMDARs are required to depolarize granule cell spines and dendrites to threshold for activating voltage-gated calcium (Ca^{2+}) channels. Indeed, Ca^{2+} channels are sufficient to evoke GABA release from granule spines (12). Furthermore, a recent study indicates that a transient potassium current (I_A) in granule dendrites attenuates fast AMPAR-mediated synaptic inputs, but permits slow NMDARs to drive DDI (16). An alternative possibility is that the high Ca^{2+} permeability of NMDARs (17) permits Ca^{2+} influx in granule spines sufficient to trigger GABA exocytosis directly. Indeed, recent studies of bulb slices in Mg^{2+}-free external solution have found that NMDAR activation of granule cells can evoke GABA release in the presence of the nonspecific Ca^{2+} channel blocker cadmium (13, 14).

While the role of Ca^{2+} channels in mitral dendrite glutamate release is not disputed, the events governing dendritic GABA release from granule cells are less clear. Most studies of DDI have used low extracellular Mg^{2+} concentration, primarily because this greatly facilitates DDI by relieving voltage-dependent inhibition of NMDARs (18). In this study, I examine the factors governing DDI in the presence of physiological levels of Mg^{2+}.

Methods

Horizontal slices (300 μm) of the olfactory bulb were prepared from 14- to 30-day-old Sprague–Dawley rats by using conventional methods (19) and viewed under differential contrast optics (BX50, Olympus). Slices were superfused with an artificial cerebrospinal fluid (ACSF) containing (in mM) 119 NaCl, 5 KCl, 2.5 $CaCl_2$, 1.3 $MgCl_2$, 1 NaH_2PO_4, 26.2 $NaHCO_3$, and 11 glucose, which was equilibrated with 95% O_2/5% CO_2. For toxin experiments, ACSF was supplemented with cytochrome *c* (0.5 mg/ml). All experiments examining DDI were performed in the presence of tetrodotoxin (TTX; 1 μM). Patch electrodes (1.5–3 MΩ) for voltage-clamp recordings of mitral cells contained (in mM) 110 CsCl, 20 Hepes, 10 tetraethylammonium (TEA) chloride, 3 MgATP, 0.5 Na_3GTP, and 0.5 EGTA (pH 7.3). In experiments using caged Ca^{2+}, EGTA was replaced with 2 mM DM-Nitrophen (the structurally identical DMNP-EDTA from Molecular Probes was used) loaded 60–70% with $CaCl_2$ and K_2ATP was substituted for MgATP. Granule cells were recorded by using an internal solution containing (in mM) 135 cesium gluconate, 8 NaCl, 10 Hepes, 12 phosphocreatine, 3 MgATP, 0.2 Na_3GTP, 0.2 EGTA, and 0.1 spermine (pH 7.3). Series resistance, which was ≈5 MΩ, was routinely compensated by >80%. Unless indicated otherwise, the holding potential was −70 mV. All experiments were performed at 30–32°C.

Voltage-clamp responses and field potentials were recorded with an Axopatch-200B and Axoclamp 2B amplifier (Axon Instruments, Foster City, CA). Mitral and granule cells were

This paper was submitted directly (Track II) to the PNAS office.

Abbreviations: GABA, γ-aminobutyric acid; DDI, dendrodendritic self-inhibition; NMDA, *N*-methyl-D-aspartate; NMDAR, NMDA receptor; AMPA, α-amino-3-hydroxy-5-methyl-4-isoxazolepropionic acid; AMPAR, AMPA receptor; TTX, tetrodotoxin; TEA, tetraethylammonium; 4-AP, 4-aminopyridine; EPSP, excitatory postsynaptic potential; EPSC, excitatory postsynaptic current; IPSC, inhibitory postsynaptic current; EPL, external plexiform layer; NBQX, 1,2,3,4-tetrahydro-6-nitro-2,3-dioxobenzo[*f*]quinoxaline-7-sulfonamide; APV, D-amino-5-phosphovaleric acid; CTZ, cyclothiazide; EGTA-AM, EGTA acetoxymethyl ester; PPF, paired pulse facilitation.

*To whom reprint requests should be addressed at: Dept. of Neuroscience, School of Medicine, University of California, San Diego, Basic Sciences Bldg., Rm. 3065, 9500 Gilman Drive, La Jolla, CA 92093-0608. E-mail: jisaacson@ucsd.edu.

The publication costs of this article were defrayed in part by page charge payment. This article must therefore be hereby marked "*advertisement*" in accordance with 18 U.S.C. §1734 solely to indicate this fact.

Article published online before print: *Proc. Natl. Acad. Sci. USA*, 10.1073/pnas.021445798. Article and publication date are at www.pnas.org/cgi/doi/10.1073/pnas.021445798

identified by their characteristic morphology. Dendritic field excitatory postsynaptic potentials (EPSPs) were evoked by using a stimulating electrode placed in the external plexiform layer (EPL). Field EPSPs were recorded by using a patch electrode containing 1 M NaCl placed parallel to the stimulating electrode in the EPL. Granule cell excitatory postsynaptic currents (EPSCs) were evoked focally by using an ACSF-filled pipette placed in the mitral layer. Synaptic responses were filtered at 1 or 2 kHz and digitized at 10 kHz (ITC-18; Instrutech, Mineola, NY). Data were acquired and analyzed by using AXOGRAPH (Axon Instruments) or routines written in IGOR (WaveMetrics; Lake Oswego, OR).

A UV flashlamp (T.I.L.L.; Martinsried, Germany) was used to photolyze caged Ca^{2+}. The ≈0.5-ms UV pulse was focused through a 60× objective onto the target mitral cell. This procedure illuminates an ≈350-μm-diameter region surrounding the mitral cell and its dendrites. DDI was quantified by measuring the current integral from 0.05 to 1.5 s after the mitral cell voltage step or UV flash. Unless indicated, traces represent the average of 5–20 sweeps. Data are shown as mean ± SEM.

Results

I first examined the nature of excitatory dendrodendritic transmission between mitral and granule cells. Previous studies of spontaneous EPSCs (11) or EPSCs evoked by focal stimulation (11, 12) suggested that both AMPARs and NMDARs mediate excitatory transmission in granule cells. Although synapses on granule cell dendrites in the EPL largely arise from dendrodendritic contacts with mitral cells, the olfactory bulb receives centrifugal inputs from cortex (4). This raises the possibility that extracellularly evoked or spontaneous, miniature EPSCs may reflect synapses other than those from mitral dendrites. To address this uncertainty, paired recordings between synaptically coupled mitral and granule cells were used to characterize unambiguously the glutamate receptors underlying dendrodendritic transmission.

Paired whole-cell recordings were performed in the presence of TTX (1 μM) to block Na^+ channels and thus prevent any contribution of axonal transmission. ACSF was supplemented with picrotoxin (100 μM) to block GABA type A ($GABA_A$) channels and extracellular Mg^{2+} concentration was reduced (100 μM). Granule cells were voltage-clamped to −60 mV and brief (10-ms) voltage steps to 0 mV were delivered to mitral cells to activate Ca^{2+} channels to trigger glutamate release. Under these conditions, mitral cells evoked a dual component EPSC in granule cells ($n = 5$, Fig. 1*A*). The fast component was abolished after application of the AMPAR antagonist 1,2,3,4-tetrahydro-6-nitro-2,3-dioxobenzo[*f*]quinoxaline-7-sulfonamide (NBQX, 10 μM), and the remaining slow component was blocked by the subsequent application of the NMDAR antagonist D-amino-5-phosphovaleric acid (APV, 100 μM). The slow, NMDAR-mediated, component was fitted by a single exponential with a time constant of 140 ± 25 ms ($n = 5$). In contrast, the AMPAR-mediated EPSC decayed rapidly with a time constant of 2.2 ± 0.3 ms ($n = 5$). These results confirm that mitral dendrite glutamate release activates slow NMDAR- and fast AMPAR-mediated EPSCs in granule cells.

To characterize further the AMPA EPSC, I used a focal stimulating electrode in the absence of TTX to activate mitral cell dendrites. In the presence of APV (100 μM), focal stimulation evoked EPSCs with rapid kinetics (decay τ 1.6 ± 0.2 ms, $n = 5$) similar to those found in cell pairs. The EPSCs reversed at ≈0 mV and showed a linear current–voltage relationship (Fig. 1*B*, $n = 3$). I next examined the actions of CTZ, a drug that slows the gating kinetics of AMPARs and prolongs the time course of AMPAR EPSCs (20, 21). Bath application of CTZ (200 μM) had no consistent effect on EPSC amplitude, but it greatly prolonged the decay time course of AMPAR EPSCs in granule cells (Fig. 1*C*). In the presence of CTZ, the EPSC time constant increased to 10.1 ± 1.0 ms ($n = 5$). In four cells, the EPSC decay in the presence of CTZ was better fit by the sum of two exponentials ($\tau_1 = 4.8 \pm 0.3$ ms and $\tau_2 = 42.5 \pm 18$ ms, $\tau_2 = 35\%$). Taken together, these results emphasize the particularly rapid kinetics of the AMPAR relative to NMDAR mediating dendritic transmission from mitral to granule cells.

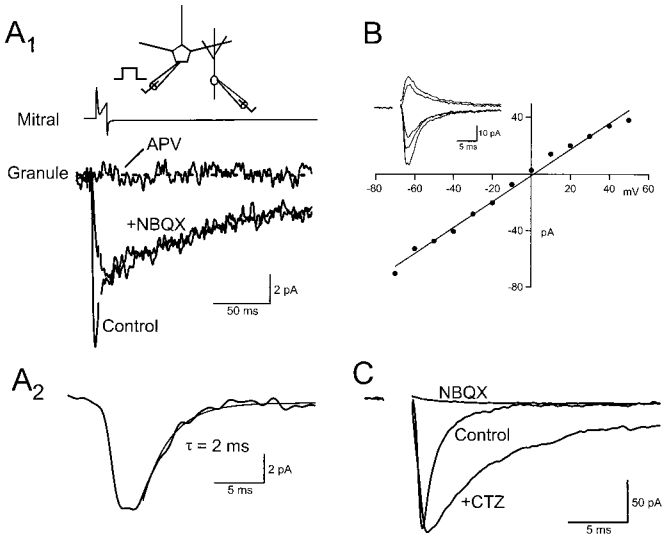

Fig. 1. AMPARs with rapid kinetics mediate fast excitatory transmission between mitral and granule dendrites. (*A*$_1$) Paired whole-cell recording between a mitral and a granule cell (shown schematically at the top) in low Mg^{2+}. Upper trace shows the voltage step (0 mV, 10 ms) applied to the mitral cell to evoke glutamate release. This generates a dual-component EPSC in the granule cell (Control). The fast component is abolished by the AMPAR antagonist (+NBQX, 10 μM), and the remaining slow component is blocked by an NMDAR antagonist (APV, 100 μM). (*A*$_2$) Digital subtraction of the response in NBQX from Control reveals the AMPAR EPSC fitted with a single exponential. (*B*) Current–voltage relationship for a granule cell AMPAR EPSC. (*C*) Granule cell AMPAR EPSC before (Control) and in the presence of cyclothiazide (CTZ, 200 μM). The EPSC in CTZ was abolished after application of NBQX.

Previous studies have shown that activation of both AMPARs and NMDARs is required to drive reciprocal DDI under normal conditions (11, 12). However, in the absence of extracellular Mg^{2+}, NMDAR activation alone is sufficient to drive GABA release from granule dendrites (11–14). These results suggested a critical role for granule cell NMDARs in reciprocal DDI and that normally AMPARs are required to provide the depolarization necessary to remove the Mg^{2+} block of NMDARs. I next examined whether AMPARs alone could be used to drive GABA release. In the presence of TTX (1 μM), reciprocal DDI was evoked by delivering brief voltage steps ($V_m = 0$ mV, 25–50 ms) to activate Ca^{2+} channels in mitral cells (12). A single voltage step generated a long-lasting barrage of inhibitory postsynaptic currents (IPSCs, Fig. 2) that are abolished by the $GABA_A$ antagonist picrotoxin (100 μM, data not shown). DDI was blocked completely after application of the NMDAR antagonists APV (100 μM) and MK-801 (20 μM) (Fig. 2*A*). In the presence of these NMDAR antagonists, CTZ (200 μM) was added to the superfusing solution. CTZ caused a complete recovery of DDI (136% ± 40% relative to control, $n = 7$), and this remaining response was abolished by NBQX (10 μM, Fig. 2*A*) or picrotoxin (not shown). Under control conditions, the decay time course of DDI was fitted by a single exponential with a time constant of 245 ± 20 ms. The decay time constant of DDI in CTZ was virtually identical (218 ± 14 ms). These results indicate that reciprocal DDI can be driven entirely by AMPARs in the presence of CTZ.

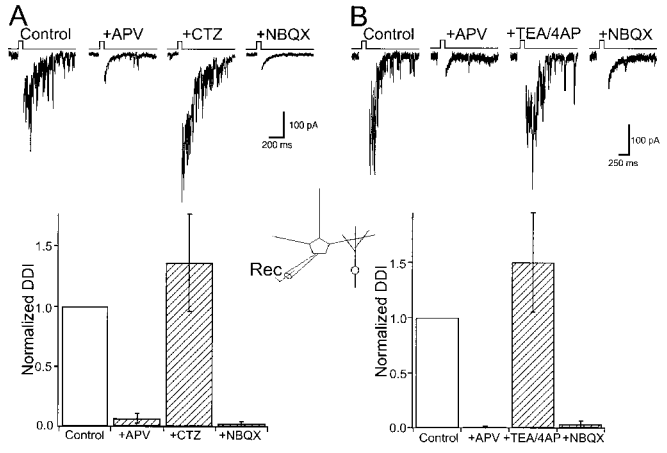

Fig. 2. AMPARs are sufficient to drive DDI evoked by mitral cell voltage steps. (*A*) (*Upper*) DDI is evoked by a brief voltage step (0 mV, 25 ms, Ca^{2+} current blanked in this and all subsequent figures) in physiological ACSF supplemented with TTX (1 μM). Single sweeps from a mitral cell before (Control) and after NMDAR antagonists were applied (+APV). In the presence of APV, CTZ restores DDI and the remaining response is abolished by NBQX. (*Lower*) Summary of all experiments ($n = 7$). (*B*) (*Upper*) Single sweeps from one cell before (Control) and after (+APV) blockade of NMDARs. In the presence of NMDAR blockers, coapplication of TEA (2 mM) and 4-aminopyridine (4AP; 200 μM) restores DDI, and the recovered response is abolished by NBQX. (*Lower*) Summary of all experiments ($n = 6$).

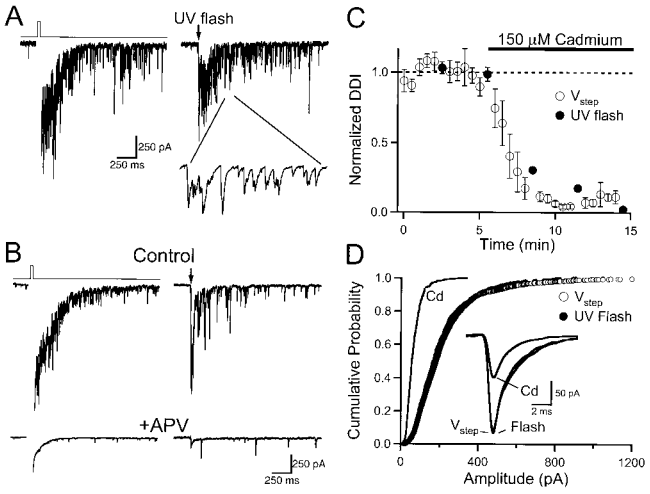

Fig. 3. DDI in physiological ACSF (1.3 mM Mg^{2+}) evoked by voltage steps and photolysis of caged Ca^{2+} in mitral cells. (*A*) Single sweeps showing that photolysis of DM-Nitrophen evokes DDI that is similar to that evoked by using a voltage step. (*Inset*) A 30-ms section of the trace, illustrating the unitary IPSCs that constitute DDI. (*B*) APV (100 μM) blocks responses to voltage steps and Ca^{2+} uncaging in the same cell. (*C*) Summary plot ($n = 6$) of the action of cadmium (150 μM) on DDI evoked by voltage steps (open circles) and photolysis of DM-Nitrophen (filled circles) in the same mitral cells. (*D*) Cumulative frequency histogram summarizing unitary IPSCs evoked by using voltage steps (open circles, $n = 1{,}958$), flash photolysis (filled circles, $n = 799$), and spontaneous events in cadmium (solid line, $n = 438$). (*Inset*) Average of ≈25 aligned IPSCs from one cell evoked by voltage steps (V_{step}), Ca^{2+} uncaging (Flash), and occurring in cadmium (Cd).

One interpretation of these results is that the slower kinetics of AMPARs in the presence of CTZ are better able to bring granule cells to threshold for activating voltage-dependent Ca^{2+} channels to trigger GABA release. To address this possibility, I examined whether DDI could be evoked by AMPARs under conditions that increase granule cell excitability. In another series of experiments, DDI was again first abolished by co-application of APV and MK-801. Potassium channels sensitive to TEA and 4-AP are generally believed to play a major role in regulating neuron excitability (22). In the presence of NMDAR antagonists, co-application of TEA (2 mM) and 4-AP (200 μM) caused a marked recovery of DDI (Fig. 2*B*, 153% ± 45% of control, $n = 6$). DDI restored by the potassium channel blockers was abolished after application of NBQX, and its decay time course was not significantly different from control (control, 187 ± 10 ms vs. TEA/4-AP, 215 ± 30 ms). These experiments support the hypothesis that AMPARs are sufficient to drive DDI under conditions that enhance granule cell excitability.

Reciprocal DDI is blocked by the inorganic Ca^{2+} channel antagonist cadmium and by ω-conotoxins that target N- and P/Q-type Ca^{2+} channels (12). However, these antagonists could block DDI simply by inhibiting glutamate release from mitral cells. I next examined the contribution of voltage-gated Ca^{2+} channels to the dendritic GABA release underlying DDI. I used caged Ca^{2+} to trigger glutamate release from mitral cells to circumvent the need for mitral dendrite Ca^{2+} channels during DDI. Mitral cells were filled with Ca^{2+}-loaded DM-Nitrophen by means of the patch pipette. A UV flashlamp was used to photolyze the caged Ca^{2+} and generate a transient increase in mitral dendrite Ca^{2+} concentration (23). In the presence of TTX and 1.3 mM Mg^{2+}, photolysis of caged Ca^{2+} in mitral cells caused a prolonged barrage of IPSCs that was similar to DDI evoked by voltage steps in the same cell (Fig. 3*A*). The DDI evoked by caged Ca^{2+} was also dependent on NMDARs, since it was abolished by APV (Fig. 3*B*, $n = 6$). UV photolysis could evoke DDI repeatedly, provided that sufficient time (≈3 min) was allowed for fresh, unphotolyzed, caged Ca^{2+} to diffuse into the mitral cell from the pipette. To assess the contribution of voltage-gated Ca^{2+} channels to granule dendrite GABA release, I examined the actions of cadmium on DDI evoked by photolysis of caged Ca^{2+}. DDI was evoked alternately by voltage steps and UV photolysis in the same cells. Cadmium (150 μM) abolished DDI evoked by both methods in parallel (Fig. 3, $n = 6$).

I next examined the individual synaptic events (Fig. 3*A Inset*) constituting reciprocal DDI. Unitary synaptic events with rise-times <1 ms, which represented the majority of IPSCs, were selected for analysis. The average amplitude of IPSCs evoked after the mitral cell voltage step was 229 ± 34 pA ($n = 6$ cells). The amplitudes of IPSCs evoked by photolysis in these same cells averaged 231 ± 38 pA. In all six cells, the amplitude distributions of IPSCs elicited by voltage steps were identical to those evoked by using caged Ca^{2+} (Fig. 3*D*, Kolmogorov–Smirnov test, $P > 0.05$). This observation provides further evidence that the synaptic events generated by voltage steps and Ca^{2+} uncaging are equivalent. Synaptic currents recorded in the presence of cadmium are generally thought to reflect quantal events caused by the spontaneous fusion of individual vesicles at presynaptic release sites (24). In the same mitral cells, the amplitudes of spontaneous IPSCs in the presence of cadmium (150 μM) averaged 69 ± 6 pA (Fig. 3*D*, $n = 4$ cells). Taken together, these results indicate that the unitary events evoked during DDI are composed of multiple quanta.

In addition to its action on Ca^{2+} channels, cadmium has been found to block neuronal NMDARs (25). This raises the possibility that cadmium may block the responses to caged Ca^{2+} by direct inhibition of granule cell NMDARs. To address this possibility, I examined the actions of cadmium (200 μM) on NMDARs in granule cells. Granule cells were voltage-clamped to −50 mV in the presence of picrotoxin (100 μM), and NMDA (100 μM) was applied focally onto their proximal dendrites by puffer pipette (50-ms pulse). Under these conditions, cadmium caused only a modest reduction in NMDAR-mediated currents in granule cells (16% ± 8%, $n = 6$). It is therefore unlikely that

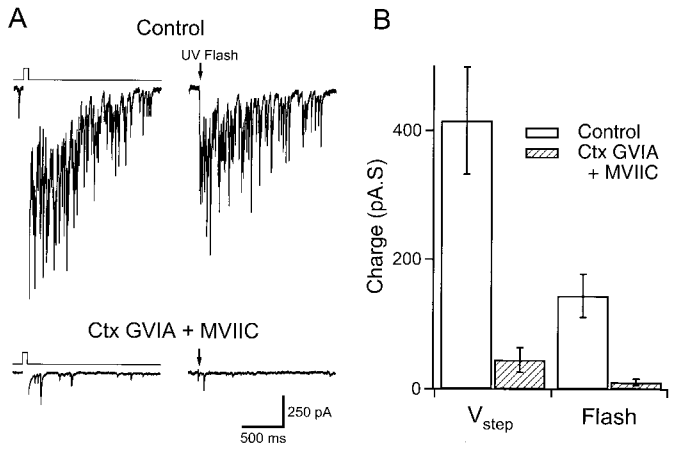

Fig. 4. ω-Conotoxins block DDI evoked by voltage steps and Ca^{2+} uncaging in the same mitral cells. (*A*) (*Upper*) Single sweeps showing responses to a voltage step and UV flash in a control cell. (*Lower*) Lack of DDI in a slice treated with ω-conotoxins (Ctx) GVIA and MVIIC. (*B*) Summary of charge transfer underlying DDI from control cells ($n = 10$) and those treated with ω-conotoxins ($n = 12$).

cadmium blocks dendritic GABA release by means of a direct inhibition of NMDARs.

Transmitter release at axonal nerve endings is triggered largely by high-voltage-activated Ca^{2+} channels sensitive to ω-conotoxins (26). N-type channels are blocked by ω-conotoxin GVIA, whereas both N- and P/Q-type channels are sensitive to ω-conotoxin MVIIC. To confirm the role of Ca^{2+} channels in reciprocal DDI, I examined the actions of these channel toxins on responses to voltage steps and Ca^{2+} uncaging in mitral cells. Slices were incubated for 1 h in ACSF supplemented with ω-conotoxin MVIIC (10 μM) and ω-conotoxin GVIA (2 μM). During recording, slices were superfused with ACSF containing both toxins (5 and 1 μM, respectively). Recordings from toxin-treated slices were interleaved with recordings from naïve slices as a control. In control recordings, DDI evoked with voltage steps averaged 415 $\pm$ 83 pA·s ($n = 10$, Fig. 4). In toxin-treated slices, DDI triggered by voltage steps was significantly less (45 $\pm$ 19 pA·s, $n = 12$). The charge transfer during DDI evoked by photolysis of caged Ca^{2+} was 144 $\pm$ 33 pA·s in the same control slices. In the presence of conotoxins, the response to flash photolysis was reduced markedly to 11 $\pm$ 5 pA·s. These results indicate an important role for high-voltage-activated Ca^{2+} channels in granule dendrite GABA release during reciprocal DDI.

I next considered whether the channels that regulate GABA release from granule dendrites were near or far from vesicle release sites. The sensitivity of transmitter release to exogenous Ca^{2+} buffers is typically used to probe the relationship between the sites of Ca^{2+} entry and the machinery underlying exocytosis. For example, only Ca^{2+} chelators that have very rapid Ca^{2+} binding kinetics [e.g., 1,2-bis(2-aminophenoxy)ethane-*N,N,N′,N′*-tetraacetate (BAPTA)] can abolish transmitter release (27, 28). In contrast, EGTA (which has similar affinity for Ca^{2+}, but slow binding kinetics) is often less effective at blocking single evoked synaptic responses. EGTA does, however, greatly reduce paired pulse facilitation, a presynaptic form of plasticity that reflects an enhancement of transmitter release caused by the accumulation of residual Ca^{2+} in the nerve terminal (29). Sensitivity to EGTA can therefore be used to determine whether there is a tight coupling between the site of Ca^{2+} entry and vesicle release machinery.

EGTA acetoxymethyl ester (EGTA-AM) is a membrane-permeant form of the chelator that introduces the Ca^{2+} buffer into neuronal compartments. Bath-applied EGTA-AM freely enters cells, where it is deesterified, rendered cell-impermeant, and accumulates intracellularly (30). Thus, levels of intracellular EGTA can far exceed the concentration of the bath-applied AM form. To determine the effectiveness of EGTA-AM in the olfactory bulb, I first studied its actions on field EPSPs evoked by stimulation in the EPL of the slice in the absence of TTX (Fig. 5*A*). Dendrodendritic synapses are highly enriched, relative to centrifugal inputs, in the EPL, and field EPSPs are thought to represent dendritic glutamate release onto granule cells (31). Paired pulse stimulation (50-ms interval) caused a clear facilitation of the field EPSP (Fig. 5*A*) and the synaptic responses were abolished by NBQX (not shown). Bath application of EGTA-AM (200 μM) did not effect the amplitude of the first EPSP, but greatly reduced the amplitude of the second EPSP (Fig. 5*A*). On average, paired pulse facilitation (PPF = EPSP2/EPSP1) was 1.46 $\pm$ 0.13 (Fig. 5*B*, $n = 5$) under control conditions. Facilitation was greatly reduced after application of EGTA-AM, and the blockade of PPF persisted 30 min after washout of the drug (PPF = 1.02 $\pm$ 0.11; Fig. 5*B*). The irreversible action of EGTA-AM is expected, given its ability to sequester inside cells. These findings indicate that EGTA-AM can enter dendritic compartments in the slice. As found for axonal synapses, these findings suggest that accumulation of dendritic Ca^{2+} governs paired pulse facilitation of glutamate release from mitral dendrites.

A previous study found that reciprocal DDI persisted after loading mitral cells with a high concentration of EGTA (20 mM) by means of the patch pipette (12). This observation indicated a tight coupling between Ca^{2+} channels and the machinery regulating glutamate release from mitral dendrites. What is the relationship between Ca^{2+} entry and the relevant release apparatus governing GABA exocytosis from granule spines? To address this question, I studied the actions of EGTA-AM on reciprocal DDI. In physiological extracellular Mg^{2+}, EGTA-AM (200 μM) was bath-applied for 10 min and the responses before and 5 min after washout of the drug were compared (Fig. 5*C*, $n = 4$). EGTA-AM did not have any consistent effects on the amplitude or time course of DDI under these conditions. I next studied the actions of EGTA-AM on DDI in ACSF containing no added Mg^{2+}, conditions under which DDI is driven entirely by NMDAR activation of granule cells. Although self-excitation attributable to NMDAR activation of mitral cells can be observed under these conditions (32–34), the vast majority of the charge after voltage steps is attributable to $GABA_AR$ IPSCs. EGTA-AM (200 μM) caused a small ($\approx$24%) reduction in DDI (Fig. 5*D*, $n = 10$). In contrast to its irreversible block of PPF, DDI recovered to control levels shortly after washout of EGTA-AM (Fig. 5*D*). EGTA-AM caused a similar, transient depression of DDI in normal ACSF (not shown). The modest action of EGTA-AM on DDI suggests a tight coupling between the sites of Ca^{2+} influx and exocytosis in granule spines.

Discussion

In this study I explored the mechanisms governing GABA release from granule cell dendrites during reciprocal dendrodendritic inhibition. In paired recordings of mitral and granule cells I found that AMPARs with fast kinetics and slow NMDARs mediate transmission from mitral to granule dendrites. In physiological concentrations of Mg^{2+}, NMDARs have an important role in DDI. However, AMPARs alone are sufficient to drive granule dendrite GABA release under conditions that increase granule cell excitability or prolong the time course of AMPAR-mediated EPSCs. Using caged Ca^{2+} to trigger glutamate release from mitral dendrites, I found that voltage-gated Ca^{2+} channels are required for granule dendrite GABA release during reciprocal DDI. Furthermore, the Ca^{2+} source triggering GABA release is tightly coupled to release zones in granule cell dendritic spines.

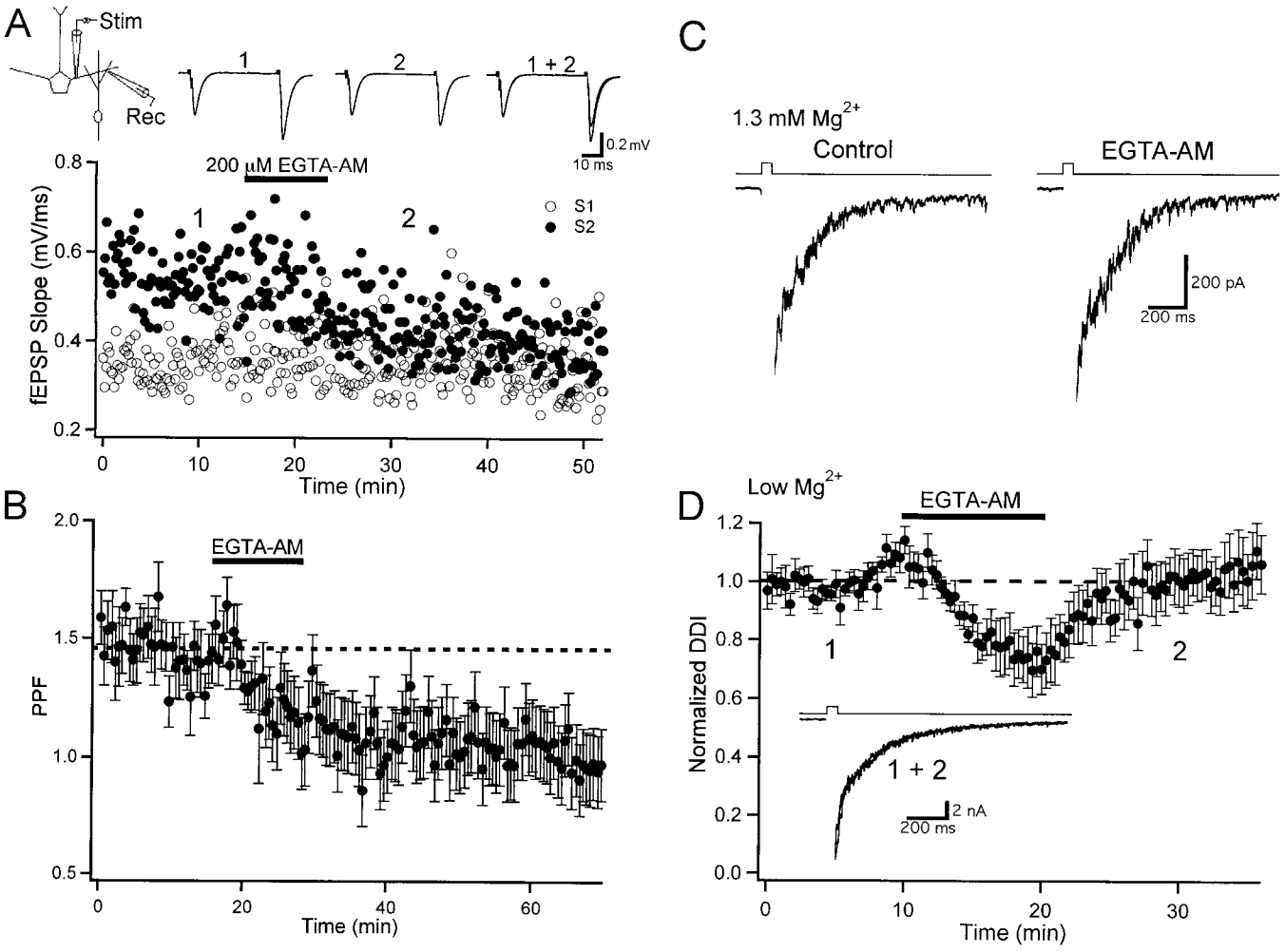

Fig. 5. Actions of EGTA-AM on dendrodendritic transmission. (*A*) Field EPSPs were evoked and recorded in the dendritic layer of the slice in the absence of TTX. Paired pulse stimulation (50-ms ISI) revealed paired pulse facilitation. The slopes of the first (S1, open circles) and second (S2, filled circles) EPSPs are plotted from one cell. Traces are taken from the times (1 and 2) indicated on the graph. EGTA-AM (200 μM) reduced the slope of S2 but had no effect on S1. (*B*) Summary plot of the effect of EGTA-AM (200 μM) on paired pulse facilitation (PPF; $n = 5$). (*C*) DDI in normal ACSF is unaffected by EGTA-AM. Traces show responses form a representative cell before (Control) and after application of EGTA-AM. (*D*) Summary plot ($n = 12$) of the actions of EGTA-AM (200 μM) on DDI in Mg^{2+}-free ACSF. (*Inset*) Responses from one cell recorded at the times indicated on the plot.

Paired recordings confirmed that both AMPA and NMDARs mediate excitatory transmission from mitral to granule dendrites. The AMPAR component was brief (decay $\tau \approx 2$ ms) compared with the NMDAR EPSC ($\tau \approx 150$ ms). AMPAR EPSCs in granule cells had a linear current–voltage relationship at positive membrane potentials. Native AMPARs are assembled from four subunits, GluR1–GluR4 (35), and immunogold labeling indicates that all four subunits are expressed on granule spines (15). AMPARs lacking GluR2 are highly permeable to Ca^{2+} and show marked inward rectification (35). The lack of rectification of the granule cell EPSC indicates that AMPARs on granule spines contain functional GluR2 subunits.

Reciprocal DDI was abolished in the presence of NMDAR antagonists. Given that both AMPARs and NMDARs mediate dendrodendritic excitatory transmission onto granule cells, why are NMDARs particularly effective at triggering GABA release? One possibility reflects the distinctly different kinetics of the two receptors. In support of this hypothesis, CTZ, which prolonged AMPAR kinetics, restored reciprocal DDI in the presence of NMDAR blockers. This finding provides direct evidence that the time course of excitatory synaptic input to granule cells is critical for driving GABA release.

I next considered the possibility that the slow kinetics of NMDARs are required to bring granule spines and/or dendrites to threshold for activating voltage-gated Ca^{2+} channels to trigger GABA release. If this were the case, than raising granule cell excitability would increase the likelihood that rapid AMPAR EPSCs could trigger GABA release. Indeed, DDI was restored in the presence of NMDAR antagonists by the K^+ channel blockers TEA and 4-AP. These findings support recent evidence indicating that A-type K^+ channels in granule dendrites selectively filter rapid AMPAR EPSCs (16). In that study, 6 mM 4-AP augmented lateral and reciprocal IPSCs and the inhibitory responses in 4-AP were less sensitive to APV than under control conditions. The results of the present study show that reciprocal DDI, reflecting local activation of granule spines, can be driven entirely by AMPARs after block of granule cell K^+ channels.

A significant feature of DDI is the slow time course of GABA release after mitral cell activation. Indeed, the slow time course of DDI is similar to the slow decay of NMDAR-mediated EPSCs in granule cells. It is tempting to speculate that this implies a direct causal relationship between NMDAR Ca^{2+} influx and granule dendrite GABA release. However, in the absence of NMDAR activation, DDI in CTZ or K^+ channel blockers had

equally slow kinetics. Furthermore, even when prolonged by CTZ, decay times of AMPAR EPSCs were still briefer than NMDAR EPSCs in granule cells. Taken together, these results suggest that properties intrinsic to granule cell dendrites, such as voltage-dependent conductances, regulate the time course of reciprocal DDI.

Photolysis of caged Ca^{2+} in mitral cell dendrites elicited DDI that was virtually identical to responses evoked by voltage steps in the same cells. I found in physiological Mg^{2+} that cadmium (150 μM) blocked reciprocal DDI evoked by voltage steps and Ca^{2+} uncaging in parallel. This result suggests a major role for voltage-gated Ca^{2+} channels as the primary source of Ca^{2+} for GABA release from granule spines.

I also examined the unitary IPSCs underlying feedback inhibition. On average, the IPSCs evoked by voltage steps and Ca^{2+} uncaging were three to four times larger in amplitude than the "quantal" events recorded in the presence of cadmium. One possibility is that $GABA_A$ receptors on mitral cells are not saturated by the contents of a single vesicle. In this case, multivesicular release at single spines may generate the large-amplitude events triggered by mitral cell glutamate release. Alternatively, the evoked IPSCs could represent the synchronous activation of several release sites from a granule dendrite making multiple contacts onto a mitral cell. A dendritic Ca^{2+} spike in granule cells could provide a mechanism for synchronous release across multiple spines. Indeed, this mechanism has been proposed to account for the lateral inhibition observed in TTX between pairs of mitral cells (12).

Experiments using ω-conotoxins yielded further evidence indicating a role for Ca^{2+} channels in dendritic GABA release. Pretreatment with ω-conotoxins GVIA and MVIIC blocked strongly DDI evoked by both voltage steps and photolysis of caged Ca^{2+}. The selective action of these toxins indicates that high-voltage-activated Ca^{2+} channels of the N- and/or P/Q-classes govern GABA release from granule spines during DDI. These findings are consistent with previous results showing that both N- and P/Q-type channels are important for DDI (12) and do not exclude a role for these channels in mitral cell glutamate release.

Although I found that DDI could be evoked readily by Ca^{2+} uncaging in physiological ACSF, a recent study using DM-Nitrophen in mitral cells reported different results (13). Chen *et al.* were unable to detect DDI produced by Ca^{2+} uncaging unless Mg^{2+} was removed from the extracellular solution. Although different UV illumination systems were used in these two studies, I have no obvious explanation for this difference. Chen *et al.* (13) found that DDI evoked by photolysis of DM-Nitrophen in Mg^{2+}-free ACSF was only modestly inhibited after addition of cadmium (100 μM) and nickel (100 μM). Similarly, another study (14) of bulb slices in Mg^{2+}-free ACSF found that mitral cell IPSCs could be evoked by using focal NMDA application in the presence of cadmium (100–200 μM). These findings were interpreted as indicating an important role for Ca^{2+} influx via NMDARs, rather than voltage-gated Ca^{2+} channels, in triggering GABA release.

I studied the actions of EGTA-AM on field EPSPs in the EPL that represent glutamatergic inputs from mitral to granule dendrites. EGTA-AM abolished paired pulse facilitation of dendritic EPSPs in the olfactory bulb. This result indicates that residual Ca^{2+} accumulation in mitral dendrites mediates short-term synaptic plasticity.

Anatomical studies have consistently noted that postsynaptic densities are segregated spatially from active zones in granule spines (15, 36). These studies indicate that there can be a significant distance ($\approx$1 μm) between glutamate receptors and the vesicle release apparatus. Indeed, an immunogold electron microscopy study indicates that NMDARs and AMPARs are highly localized at postsynaptic junctions and excluded from GABA release sites in granule spines (15). It is typically believed that fast transmitter release requires high concentrations (>100 μM) of Ca^{2+} in local microdomains at the site of exocytosis (refs. 26 and 27, but see refs. 37 and 38). In agreement with this hypothesis, reciprocal DDI was largely unaffected after application of EGTA-AM. The modest, reversible, reduction in DDI may reflect the fact that extracellularly applied Ca^{2+} chelators are competitive blockers of NMDARs (39). The rapid recovery of DDI is unlikely to be caused by a loss of intracellular EGTA because EGTA-AM had an irreversible action on PPF of field EPSPs. I cannot rule out the possibility that the EGTA in granule spines was saturated by Ca^{2+} influx during DDI. However, the lack of effect of EGTA is consistent with the hypothesis that channels providing the source of Ca^{2+} for GABA exocytosis must be in close proximity to the site of transmitter release. Local Ca^{2+} channels at GABA release sites (12) could serve this purpose.

In summary, it has been suggested that Ca^{2+} influx through NMDARs can trigger directly GABA release from granule cell dendrites in the olfactory bulb (13, 14). However, these studies were performed under conditions (Mg^{2+}-free ACSF) that greatly enhance the contribution of NMDARs to DDI. In contrast, other studies have suggested that NMDARs are particularly adept at activating voltage-gated Ca^{2+} channels in granule cell spines and dendrites (11, 12, 16). Although I cannot exclude a facilitory role for Ca^{2+} influx through NMDARs under some circumstances, this study using physiological levels of Mg^{2+} indicates a major role for voltage-gated Ca^{2+} channels in governing GABA exocytosis during reciprocal DDI.

I thank Jane Sullivan for advice and helpful suggestions. This work was supported by a Burroughs Wellcome Fund Career Award, McKnight Scholar Award, and University of California at San Diego start-up funds.

1. Cheramy, A., Leviel, V. & Glowinski, J. (1981) *Nature (London)* **289,** 537–542.
2. Simmons, M. L., Terman, G. W., Gibbs, S. M. & Chavkin, C. (1995) *Neuron* **14,** 1265–1272.
3. Zilberter, Y., Kaiser, K. M. & Sakmann, B. (1999) *Neuron* **24,** 979–988.
4. Shepherd, G. M. & Greer, C. A. (1998) in *The Synaptic Organization of the Brain* (Oxford Univ. Press, New York), pp. 159–203.
5. Nicoll, R. A. (1969) *Brain Res.* **14,** 157–172.
6. Nowycky, M. C., Mori, K. & Shepherd, G. M. (1981) *J. Neurophysiol.* **46,** 639–648.
7. Jahr, C. E. & Nicoll, R. A. (1980) *Science* **207,** 1473–1475.
8. Rall, W., Shepherd, G. M., Reese, T. S. & Brightman, M. W. (1966) *Exp. Neurol.* **14,** 44–56.
9. Wellis, D. P. & Kauer, J. S. (1993) *J. Physiol.* **469,** 315–339.
10. Mori, K., Nagao, H. & Yoshihara, Y. (1999) *Science* **286,** 711–715.
11. Schoppa, N. E., Kinzie, J. M., Sahara, Y., Segerson, T. P. & Westbrook, G. L. (1998) *J. Neurosci.* **18,** 6790–6802.
12. Isaacson, J. S. & Strowbridge, B. (1998) *Neuron* **20,** 749–761.
13. Chen, W. R., Xiong, W. & Shepherd, G. M. (2000) *Neuron* **25,** 625–633.
14. Halabisky, B., Friedman, D., Radojicic, M. & Strowbridge, B. W. (2000) *J. Neurosci.* **20,** 5124–5134.
15. Sassoe-Pognetto, M. & Ottersen, O. P. (2000) *J. Neurosci.* **20,** 2192–2201.
16. Schoppa, N. E. & Westbrook, G. L. (1999) *Nat. Neurosci.* **2,** 1106–1113.
17. Mayer, M. L. & Westbrook, G. L. (1987) *J. Physiol. (London)* **394,** 501–527.
18. Mayer, M. L., Westbrook, G. L. & Guthrie, P. B. (1984) *Nature (London)* **309,** 261–263.
19. Isaacson, J. S. & Walmsley, B. (1995) *J. Neurophysiol.* **73,** 964–973.
20. Isaacson, J. S. & Walmsley, B. (1996) *J. Neurophysiol.* **76,** 1566–1571.
21. Partin, K. M., Bowie, D. & Mayer, M. L. (1995) *Neuron* **14,** 833–843.
22. Hille, B. (1992) *Ionic Channels of Excitable Membranes* (Sinauer, Sunderland, MA).
23. Zucker, R. S. (1993) *Cell Calcium* **14,** 87–100.
24. Katz, B. (1969) *The Release of Neural Transmitter Substances* (Liverpool Univ. Press, Liverpool, U.K.).
25. Mayer, M. L., Vyklicky, L., Jr., & Westbrook, G. L. (1989) *J. Physiol. (London)* **415,** 329–350.
26. Dunlap, K., Luebke, J. I. & Turner, T. J. (1995) *Trends Neurosci.* **18,** 89–98.
27. Adler, E. M., Augustine, G. J., Duffy, S. N. & Charlton, M. P. (1991) *J. Neurosci.* **11,** 1496–1507.
28. Pavlidis, P. & Madison, D. V. (1999) *J. Neurophysiol.* **81,** 2787–2797.
29. Atluri, P. P. & Regehr, W. G. (1996) *J. Neurosci.* **16,** 5661–5671.
30. Tsien, R. Y. (1981) *Nature (London)* **290,** 527–528.
31. Aroniadou-Anderjaska, V., Ennis, M. & Shipley, M. T. (1999) *J. Neurophysiol.* **81,** 15–28.
32. Isaacson, J. S. (1999) *Neuron* **23,** 377–384.
33. Aroniadou-Anderjaska, V., Ennis, M. & Shipley, M. T. (1999) *J. Neurophysiol.* **82,** 489–494.
34. Friedman, D. & Strowbridge, B. W. (2000) *J. Neurophysiol.* **84,** 39–50.
35. Hollmann, M. & Heinemann, S. (1994) *Annu. Rev. Neurosci.* **17,** 31–108.
36. Price, J. L. & Powell, T. P. S. (1970) *J. Cell Sci.* **7,** 125–155.
37. Schneggenburger, R. & Neher, E. (2000) *Nature (London)* **406,** 889–893.
38. Bollmann, J. H., Sakmann, B. & Borst, J. G. (2000) *Science* **289,** 953–957.
39. Chen, N., Murphy, T. H. & Raymond, L. A. (2000) *J. Neurophysiol.* **84,** 693–697.